International Journal of Modelling and Simulation

ISSN: 0228-6203 (Print) 1925-7082 (Online) Journal homepage: http://www.tandfonline.com/loi/tjms20

Modelling and Simulation of a Hybrid Vehicle Using Direct Torque Control of Induction Motor

M. Vasudevan, R. Arumugam & S. Paramasivam

To cite this article: M. Vasudevan, R. Arumugam & S. Paramasivam (2007) Modelling and Simulation of a Hybrid Vehicle Using Direct Torque Control of Induction Motor, International Journal of Modelling and Simulation, 27:1, 80-88

To link to this article: http://dx.doi.org/10.1080/02286203.2007.11442403

Published online: 15 Jul 2015.

MODELLING AND SIMULATION OF A HYBRID VEHICLE USING DIRECT TORQUE CONTROL OF INDUCTION MOTOR

M. Vasudevan,* R. Arumugam,* and S. Paramasivam*

Abstract

The authors develop and present a new model of a hybrid vehicle and control strategy. The hybrid vehicle is a general class of vehicles in which the prime power and the driveline are decoupled. The configuration considered in this paper consists of a diesel engine driving a permanent magnet generator that supplies rectified power to a DC link, which in turn supplies power through an inverter to an induction motor for traction. The control system proposed is hierarchical with controllers at the component, subsystem, and system level. Direct torque control (DTC) algorithm is applied to control the induction motor. The subsystem controllers consist of feedback control loops encompassing sliding mode, bang-bang, and conventional control laws. At the system level, a logic controller balances source and loads on the system bus. All models and controllers are simulated using MATLAB and SIMULINK computer program. The performance and scalability of each subsystem controller is demonstrated in stand-alone computer simulations. The modelling and control strategy proposed in this paper provides a robust, scalable system model for simulating the effects of standard driving cycles on the power system of a given vehicle configuration over long time scales.

Key Words

Hybrid vehicle, induction motor, direct torque control, vehicle dynamics, FUDS data

1. Introduction

Electric vehicles are those powered by one or more energy storage systems, which must be charged and recharged by a power source external to the vehicle [1]. Conventional vehicles are powered by a combustion engine or other source of power derived from the consumption of fuel. Hybrid electric vehicles combine elements of both electric and conventional vehicles. That is, they have two or more sources of power, one or more derived from fuel consumption and one or more derived from rechargeable energy storage systems [2]. The advantages of them are potential for lower emissions, increased efficiency of operations, and greatly improved performance of the electrically distributed power system over its mechanically distributed counterpart [3]. The objective of this paper is to provide a comprehensive system model and control strategy for the most commonly proposed hybrid electrical vehicle configurations.

* Department of Electrical and Electronics Engineering, College of Engineering, Anna University, Chennai, India; e-mail: vasumame@yahoo.com, arumugam@annauniv.edu, paramsathya@yahoo.com

Recommended by Prof. Behrooz Fallahi
(paper no. 205-4523)

2. System Configuration

The system configured as shown in Fig. 1 can be divided into subsystems; the architecture to be studied here will thus consist of a main power supply subsystem, a load-leveling power supply subsystem, a vehicle speed subsystem, and a DC link connecting the subsystems. The main power supply subsystem consists of a diesel engine, a three-phase AC permanent magnet synchronous generator, and a pulse width modulated (PWM) controlled converter to couple the generator to the DC link. The load-leveling power supply subsystem is simply a flywheel battery composed of a mechanical flywheel, a three-phase AC permanent magnet synchronous machine, and a PWM controlled converter to couple the machine to the DC link. Finally, the vehicle speed subsystem consists of a PWM controlled converter to couple the traction motor to the DC link, a three-phase induction motor, which is used as traction motor, and the vehicle dynamics. This paper proposes the development of computer models to represent the vehicle power system on the order of the system-level dynamics and also the design of a robust stable control system to effectively manage the power flow through this system.

We propose to manage the power flow in the vehicle by using a hierarchical control scheme. At the top level of the control system, an intuitive energy management controller will be used to control the various subsystems in order to balance the loads with the sources and to prevent machines from exceeding rated power. The second level of the control hierarchy consists of controllers at the subsystem level. The main power supply subsystem, consisting of the prime mover, main generator, and mechanical and electrical couplings, is proposed to be controlled with a combination of sliding mode control (SMC) to control

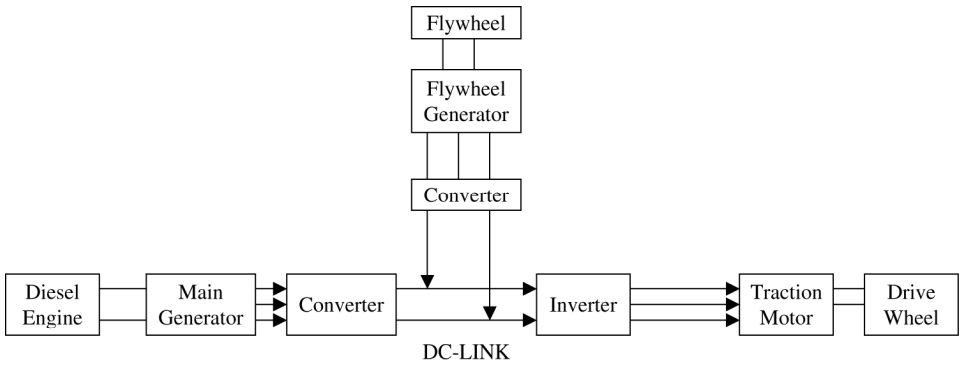

Figure 1. System configuration.

engine speed and feed forward/feedback control to control generated DC current. The load-leveling power supply subsystem controller will be a simple on/off controller to control the flywheel battery state of charge (SOC). Finally, a time-optimal bang-bang control algorithm will be used to simulate a human driver attempting to control the vehicle speed. The third and lowest level of control is control of the AC machines on the order of the electrical transients. Each of the machines is to be controlled with torque vector control, in which the flux and torque are decoupled and controlled independently. The controller solution proposed here will be demonstrated through stand-alone subsystem computer simulations.

3. Modelling of the System

Modelling of the system involves the complete design of electrical machines and mechanical decoupling. The major electrical machines involved in hybrid electric vehicle are permanent magnet synchronous machine (PMSM) and an induction machine. Controllers for these electric machines are designed for the vehicle from the machine modelling.

3.1 Model of PMSM

The PMSM is used in the vehicle model as the main generator and as the flywheel machine, which is a two-pole, three-phase, star-connected, symmetrical permanent magnet synchronous machine [4, 5]. The model used in the vehicle simulation does not consider electrical transients, as these transients occur on a time scale much smaller than the time scale of interest. The steady-state equations are given in (1) and (2). The developed torque in the machine is given by (3).

$$v_{qs} = -R_s i_{qs} - \omega_r L_d i_{ds} + \omega_r \psi_m \tag{1}$$

$$v_{ds} = -R_s i_{ds} + \omega_r L_q i_{qs} \tag{2}$$

$$T_d = \frac{3}{2}(\psi_m i_{qs} + (L_d - L_q) i_{qs} i_{ds}) \tag{3}$$

PMSM receives as inputs v_{qs}, v_{ds} and ω_r. The controlled converter sets the voltage amplitude and frequency across the machine terminals, and the shaft coupling specifies the mechanical speed. The permanent magnet machine is responsible for specifying i_{qs} and i_{ds} to the controlled converter and T_d to the shaft coupling. In order to solve for the inputs in terms of the outputs, (1–2) can be solved together for i_{qs} and i_{ds}, resulting in (4). With these currents known, developed torque can be solved explicitly using (3).

$$\begin{Bmatrix} i_{qs} \\ i_{ds} \end{Bmatrix} = \frac{1}{R_s^2 + \omega_r^2 L_d L_q} \begin{bmatrix} -R_s & \omega_r L_d \\ -\omega_r L_q & -R_s \end{bmatrix} . \begin{Bmatrix} v_{qs} - \omega_r \psi_m \\ v_{ds} \end{Bmatrix} \tag{4}$$

3.2 Model of an Induction Machine

The motor model calculates the torque, stator flux, and shaft speed based on the measurement of two-phase currents and the intermediate circuit dc voltage [6, 7]. Torque and flux references are compared with these values, and control signals are produced using a two-level hysteresis. The optimal switching logic defines the best voltage vector based on torque and flux references [8].

The expression for the developed torque of an induction motor is:

$$T = \frac{N_p M \psi_s \psi_r \sin\delta}{\sigma L_s L_r} \tag{5}$$

where $\sigma = 1 - M^2/(L_s L_r)$, $\psi_s =$ stator flux, $\psi_r =$ rotor flux, and $\delta =$ torque angle between stator and rotor fluxes.

Under normal operating conditions, the amplitude of the working flux is kept constant at the maximum value. Hence the developed torque is proportional to the sine of the torque angle "δ" between stator and rotor fluxes, and can be controlled by suitably changing the angle "δ". As the time constant of rotor current is large compared to stator, the stator flux is accelerated or decelerated with respect to the rotor flux to change the torque angle. Stator flux is a computational quantity, which is obtained using the stator-measured current "I_s" and voltage "V_s".

$$\psi_s = \int_0^t (V_s - I_s R_s) \cdot dt \tag{6}$$

3.3 Vehicle Dynamics

The vehicle model consists only of a mass moving along a one-dimensional path. Elements included in the model are axle drag torque proportional to speed, aerodynamic drag torque proportional to the vehicle speed squared, and dry friction or rolling resistance proportional to the mass of the vehicle.

As a contained unit, the vehicle model takes as input the axle shaft torque and frictional brake torque. The outputs of the vehicle are axle shaft speed and velocity of the vehicle. Because there is only one energy-storing element in this model—the mass of the vehicle—the dynamics of the vehicle are first order. Again, this model is not intended to enable a detailed analysis of vehicle dynamic response. It is given in this form to provide a simple yet somewhat realistic load by which to judge the performance of the vehicle power system. The velocity state equation in the vehicle model is:

$$\overline{V_{veh}} = \frac{1}{M_{eff}} \left\{ \frac{T_a - b_a\omega_a - T_b}{r} - \frac{V_{veh}}{|V_{veh}|} \left[C_d \left(\frac{1}{2}\rho V_{veh}^2 \right) A + F_m \right] \right\} \quad (7)$$

where V_{veh} is the velocity of the vehicle, M_{eff} is the effective inertia of the vehicle, r is the radius of each tire, C_d is the aerodynamic drag coefficient, ρ is the density of air, A is the frontal area of the vehicle, F_m is the dry friction force, T_a is the axle shaft torque, ω_a is the axle shaft speed, b_a is the axle drag torque constant, and T_b is the frictional brake torque. Here the effective inertia of the vehicle, M_{eff}, is the mass of the vehicle in addition to the effective mass of the traction motor as propagated through the drive train. The vehicle dynamics is developed by SIMULINK package.

Other models are mechanical coupling, flywheel, and DC link. Briefly, the mechanical coupling is modelled as a simple gear with viscous drag torque. The flywheel model is a simple lumped inertia model with viscous drag torque. The equation for flywheel shaft speed is:

$$\overline{\omega}_f = \frac{1}{J_{eff}}(\tau_f - b_f\omega_f) \quad (8)$$

where ω_f is the rotational speed of the flywheel, τ_f is the external applied shaft torque, b_f is the viscous damping coefficient for flywheel drag torque, and J_{eff} is the constant effective lumped moment of inertia of the flywheel and anything rigidly connected to it. Usually when it is decided to neglect the electrical transients in one component of a system, it is necessary to neglect all electrical transients in the system. Otherwise, the transients that are modelled do not reflect the true electrical dynamics of the system. In modelling the DC link, one electrical state, the bus voltage, is included. The state equation for the system bus voltage may be derived as:

$$\overline{v_b} = \frac{1}{C_b}\left(i_{sources} - i_{sinks} - \frac{v_b}{R_b} \right) \quad (9)$$

4. Design of System Controllers

In the design of this system controller, the two most significant factors influencing the overall methodology are the necessity of a practical design and limitations on control actuators. A practical controller in this case is a controller that allows human-in-the-loop input from the driver in the form of accelerating and braking torque commands. The driver is simulated as a simple control loop in this paper but will have unpredictable dynamics in the physical system. A control system that would not be practical would be one in which the entire velocity profile of the vehicle would be required to set certain control parameters prior to operation. For instance, a full-state feedback optimal controller requires such knowledge to specify the feedback control gains as a function of time such that some system performance index is minimized. In this case, the performance of the system would be less than optimal. One method of alleviating this problem is to have decentralized subsystem controllers that only act to control their own subsystems based on power flow information provided by a top-level controller. With this approach, each subsystem controller may then be controlled by whatever control technique best suits that particular subsystem. In addition, this makes the system more modular in that additional subsystems and their associated controllers could be easily incorporated into the system model by altering only the power flow logic in the top-level controller. Because the top-level controller is responsible for the power flow management in the system, it is dubbed the Energy Management Controller. Because all power must flow in electrical form to or from the DC link, it is natural to specify the common boundary of each subsystem at this point. The Energy Management Controller is then responsible for determining the limits on power that may be drawn from or supplied to the system bus. Likewise, each subsystem controller must be able to maintain stability in spite of limited resources. Here the top-level of control is the Energy Management Controller, which is tasked with balancing the power flow on the system bus. The second level, or mid-level, of control is each subsystem controller. Finally, the lowest level of control is at the induction motor torque control level. The revelation of and justification for the particular control technique used in each instance of low-level and mid-level control is highlighted.

4.1 Vector Control of Permanent Magnet Machine

In the permanent magnet machine model, recall that the inputs to the machine (via its controlled converter) are v_{qs}^* and v_{ds}^*. It is assumed that the machine controller has access to the measured shaft speed of the machine as well. Thus, the object of the machine controller is to specify v_{qs}^* and v_{ds}^* based on τ_g^* and ω_r such that $\tau_g = \tau_g^*$. Note that in a real system, there would most likely be feedback of all the voltages and currents across the stator windings, and there would be a feedback portion of the controller that would try to drive the actual voltages and currents to their reference values. With vector control of a permanent magnet synchronous machine, maximum per

unit armature current is obtained when i_{ds} is held at zero and i_{qs} is varied to control the torque [10].

4.2 DTC of Induction Motor

The core of DTC consists of hysteresis controllers of torque and flux, optimal switching logic, and precise motor model as shown in Fig. 2. In principle, the DTC method selects one of the inverter's six voltage vectors and two zero vectors as shown in Fig. 3 in order to keep the stator flux and torque within a hysteresis band around the demand flux and torque magnitudes [9, 10]. The motor model calculates the torque, stator flux, and shaft speed based on the measurement of two-phase currents and the intermediate circuit dc voltage. Torque and flux references are compared with these values, and control signals are produced using a two-level hysteresis. The optimal switching logic defines the best voltage vector based on torque and flux references. Table 1 defines selection of voltage vectors. From the table, it is observed that C_ψ is change in flux and C_T is change in torque. The voltage vectors V_1, V_2, V_3, V_4, V_5, and V_6 are enable vectors and V_0 and V_7 are disable vectors.

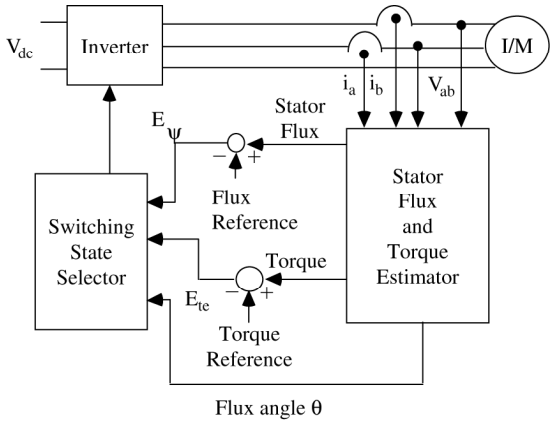

Figure 2. Model of direct torque control.

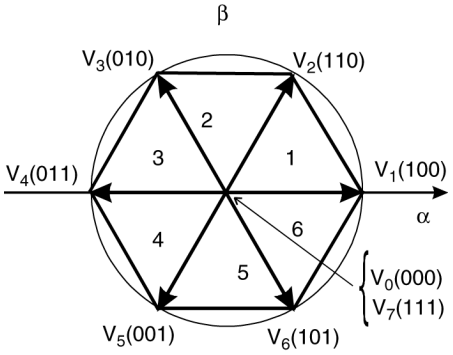

Figure 3. DTC space vectors.

4.3 Main Power Supply Subsystem

The main power supply subsystem consists of the diesel engine, mechanical coupling, permanent magnet machine, controlled converter, and permanent magnet machine vector controller. The inputs to the subsystem are system bus voltage, engine throttle position, and generator torque command. The outputs of this subsystem are engine shaft speed and generated DC current. The purpose of this subsystem is to produce a commanded DC current as efficiently as possible.

Table 1
Basic Switching

		Sector					
C_ψ	C_T	1	2	3	4	5	6
↑	↑	V_2	V_3	V_4	V_5	V_6	V_1
	0	V_0	V_0	V_0	V_0	V_0	V_0
	↓	V_6	V_1	V_2	V_3	V_4	V_5
↓	↑	V_3	V_4	V_5	V_6	V_1	V_2
	0	V_0	V_0	V_0	V_0	V_0	V_0
	↓	V_5	V_6	V_1	V_2	V_3	V_4

This controller interfaces with the lower level of control by adjusting the engine throttle setting and sending a command torque to the permanent magnet machine vector controller. This controller interfaces with the higher level of control by receiving a DC current command and specifying the amount of DC current that may be supplied to the rest of the system.

The main power supply subsystem controller uses the inputs engine shaft speed and reference and actual generated DC current to determine the appropriate values for the outputs permanent magnet machine torque command and engine throttle setting. First, the engine speed and reference DC current are used to determine the optimal engine reference speed. Next, this reference speed and the actual and reference values of DC current are used to determine the required throttle setting to produce the necessary DC current. Finally, this throttle setting and the reference and actual engine speeds are used to determine the permanent magnet machine torque command that will control the engine speed.

4.4 Vehicle Speed Subsystem

The vehicle speed subsystem consists of the induction motor, its controlled converter and direct torque controller, the mechanical coupling, and the vehicle dynamics. The inputs to this subsystem are system bus voltage and induction machine torque command, and the outputs are DC current drawn from the system bus and vehicle speed. The objective of this subsystem is to use induction motor and brake torque to control the speed of the vehicle.

5. Simulation Procedures

The computer simulation illustrates the main power supply subsystem model and controller performance. In this simulation, the bus voltage is assumed to be constant and the input to the subsystem is reference DC current. In order to test the main power supply subsystem controller,

a step input of reference DC current is applied and then removed after equilibrium has been reached. The step is from 0 to the maximum DC current that may be obtained from the main power supply subsystem. To test the scalability of the subsystem model and its controller, this test will be performed for the lowest and highest expected values of rated engine power, with all other parameters scaled. This simulation was performed in SIMULINK with the 4th-order Runge-Kutta integration routine with a fixed time step of 0.1 second. The system was simulated for 60 seconds, with the step input applied during the first 30 seconds and removed during the remaining 30 seconds.

6. Results and Discussion

The SIMULINK code for the entire vehicle system model is used in this paper. For convenience, the SIMULINK code was simulated from the MATLAB command line in a script file [11]. This script file enables a single batch process to obtain all relevant data required to evaluate the results. For simulation, 50-HP rated traction motor and engine are used. The Federal Urban Driving Schedule (FUDS) data is specified for 1372 seconds; it is required to simulate a total of 405*1372 = 555660 seconds or 154.34 hours in order to evaluate the performance index. If the vehicle model considered electrical dynamics, the required time step would be much smaller, thus making the time to simulate much longer. The general rule in simulating dynamic systems is that simulation time is inversely proportional to the integration time step. Using the maximum time step for which a stable response is obtained. Fig. 4 shows the graph of FUDS data, in which vehicle speed is in miles per hour and time is in seconds.

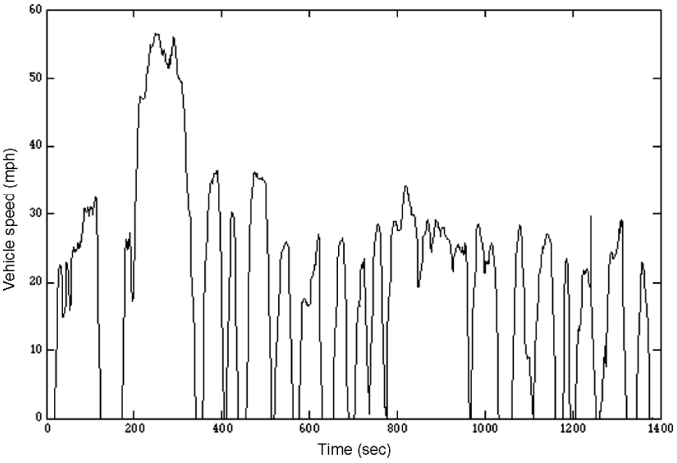

Figure 4. Federal urban drive schedule.

For the 50-HP engine configuration, the DC current response is given in Fig. 5. In this figure, the dash-dotted line represents the reference DC current and the solid line is the actual DC current produced. As seen in this figure, the steady-state error is less than the desired 2% of rated DC current. The control variable that produces this result is the engine throttle position, shown in Fig. 7. As shown in this figure, the throttle position is in nondimensional form with $\theta = 0$ corresponding to the fully closed position and $\theta = 1$ corresponding to the fully open position. The other state to be controlled in this subsystem is the engine shaft speed. Its response is shown in Fig. 6 for the 50-HP main power supply. In this figure, the reference speed shown as a dash-dotted line is actually the filtered reference speed. It is apparent from this figure that the shaft speed follows the reference speed well within the 10 rad/sec error bandwidth, as expected with a sliding mode control principle. The control input here is the generator torque, shown in Fig. 8. The trajectory of the generator torque appears to be proportional to the generated DC current. Finally, the fuel usage during this one-minute simulation is illustrated in Fig. 9. In the 1 MJ flywheel battery test, the bus voltage is maintained to within 1 volt of the reference

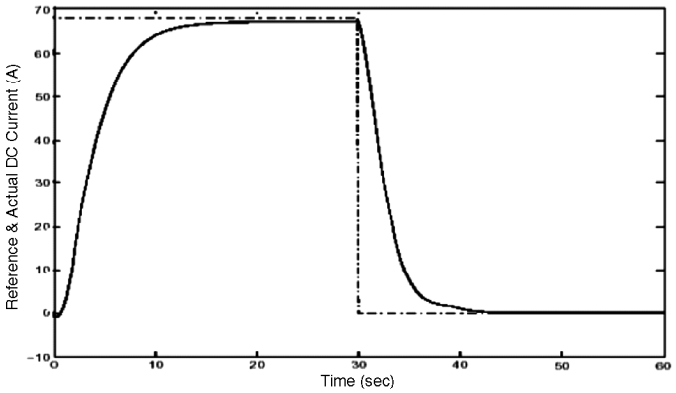

Figure 5. Generated DC current.

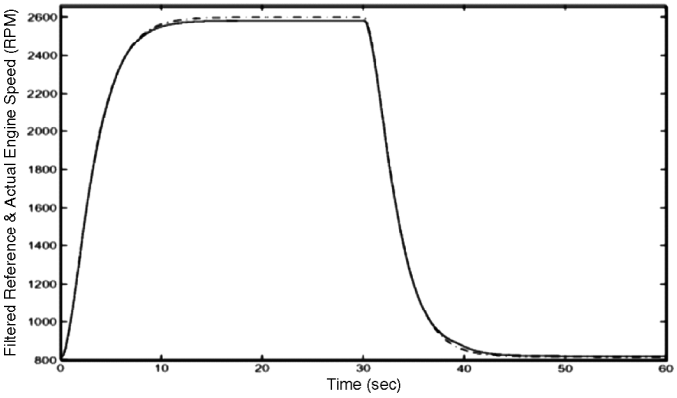

Figure 6. Engine shaft speed.

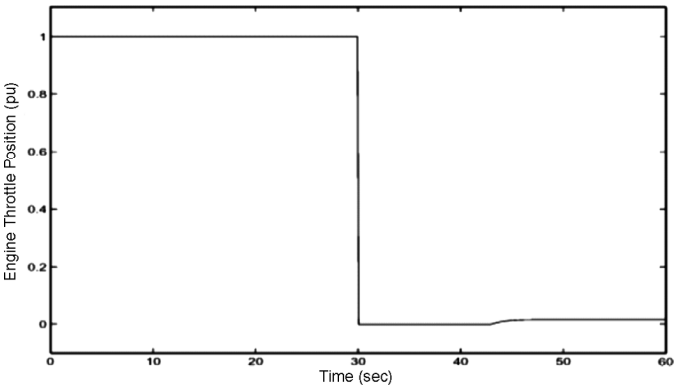

Figure 7. Engine throttle position.

value, as shown in Fig. 10. This represents a maximum error of 0.2%. In fact, if it were not for the leakage in the DC link, the voltage would be precisely maintained and the feedback portion of the voltage controller would be unnecessary. This is due to the fact that the models used in the feed forward controller are exactly the same as the models in the subsystem. The only difference is that the leakage has been neglected in the feed forward controller. The DC current produced by the flywheel battery that maintains bus voltage is shown in Fig. 12. The machine torque that was used to produce this current is given in Fig. 13. Note that the machine torque does not appear to be directly proportional to generated current as it did in the main power supply subsystem. This difference may be attributed to the rapidly varying shaft speed in the flywheel battery, which greatly affects the relationship between developed torque and generated current. The shaft speed of the flywheel, which is designed to operate at 36,000 RPM when fully charged, is shown in Fig. 11. The state of charge of the flywheel battery is the square of the nondimensional flywheel speed. The resulting flywheel battery state of charge for this test case is given in Fig. 14. From the state of charge data, it is seen that the flywheel battery requires 61 seconds to charge and 52.5 seconds to discharge. This is exactly as expected from the charge time analysis above. The difference between actual and

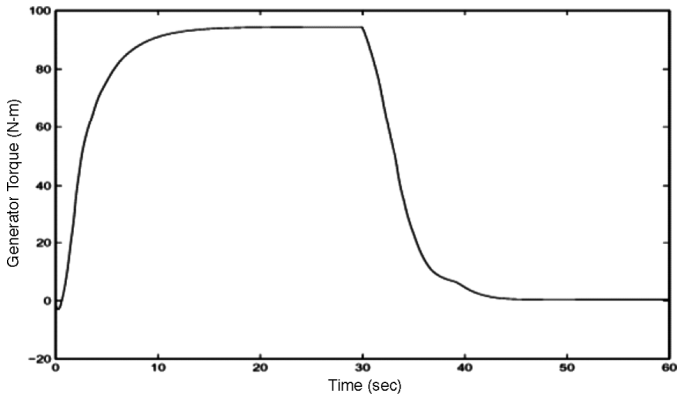

Figure 8. Generator torque.

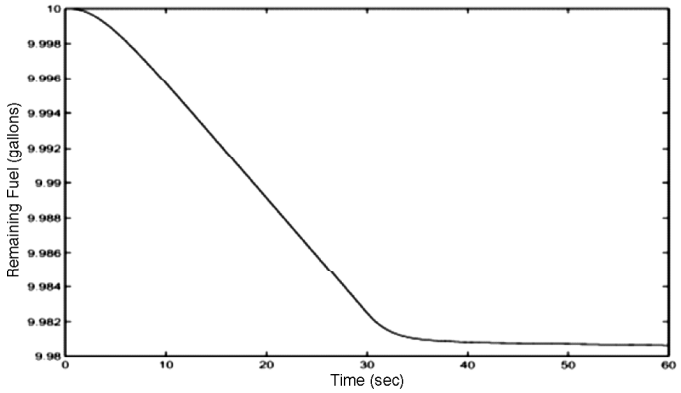

Figure 9. Engine fuel remaining.

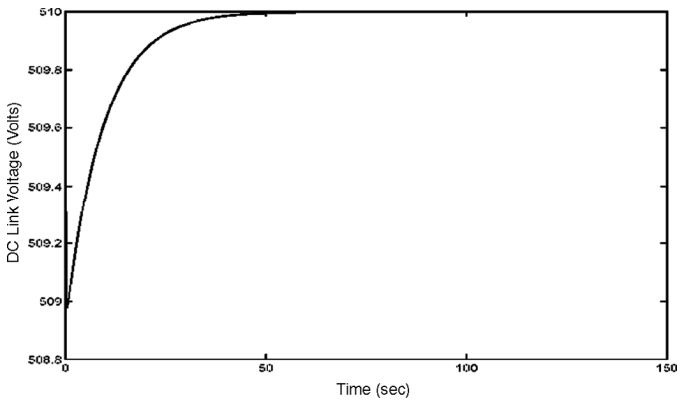

Figure 10. DC link voltage.

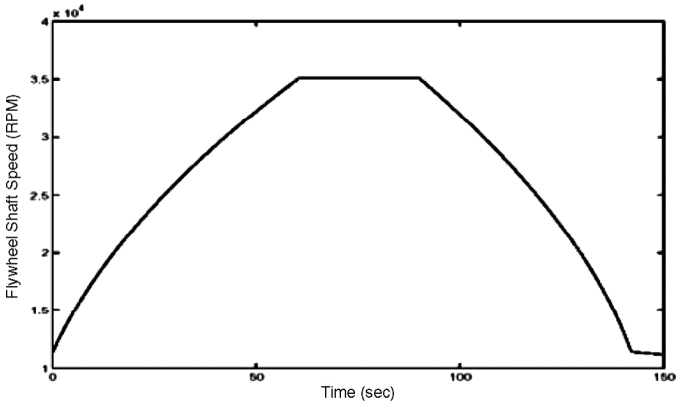

Figure 11. Flywheel speed.

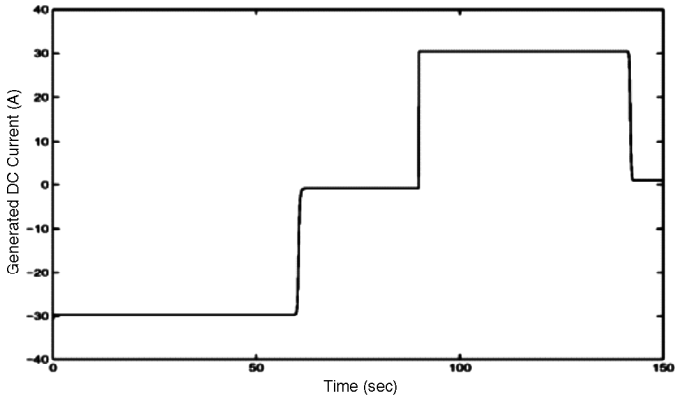

Figure 12. Generated DC current.

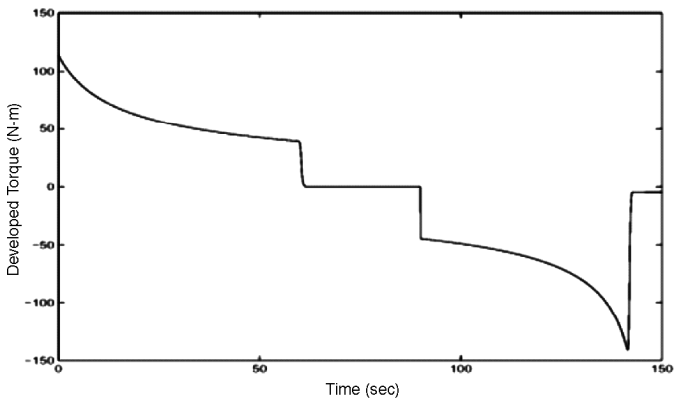

Figure 13. Torque developed.

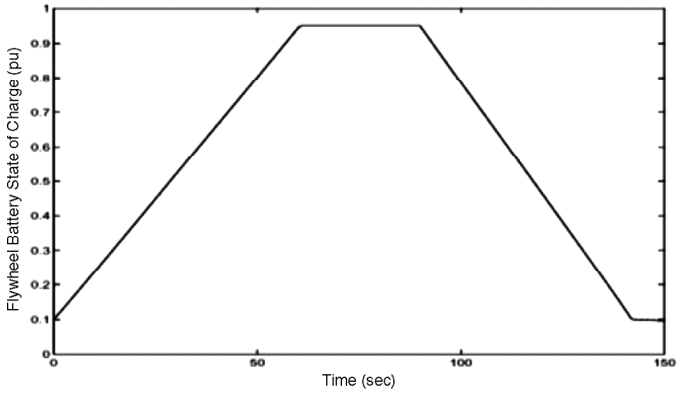

Figure 14. State of charge.

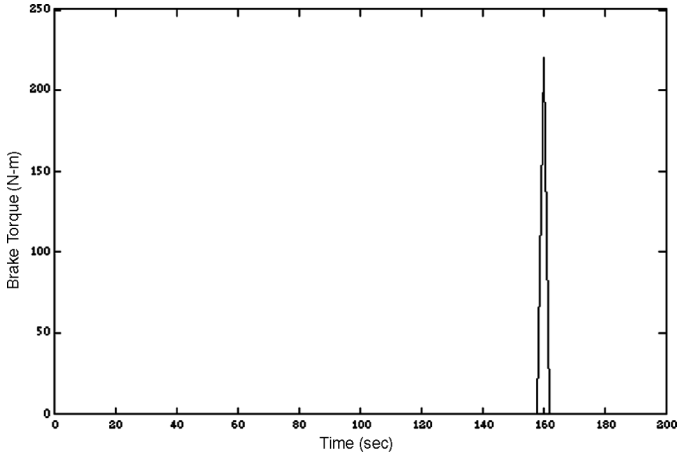

Figure 15. Mechanical brake torque.

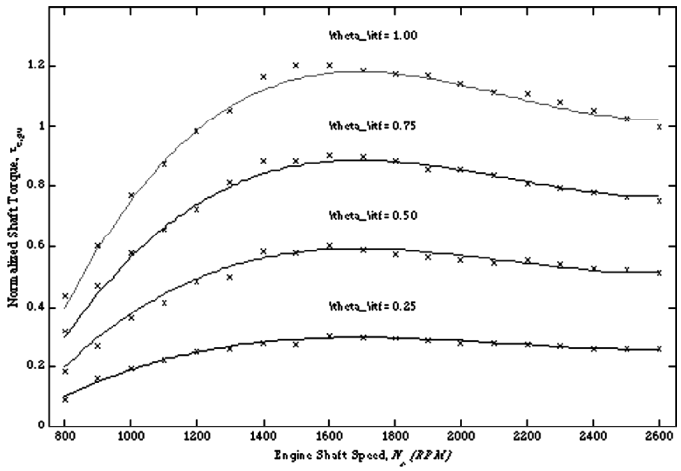

Figure 16. Engine torque curve fit results.

theoretical charge and discharge time is attributed to the fact that there are power losses in the permanent magnet machine and mechanical coupling, which prevent all of the energy entering the machine terminals from being stored in the flywheel.

Fig. 16 shows the normalized shaft torque of the engine based on the curve fit analysis. With the help of this graph, maximum normalized torque error between the design model and the truth model can be calculated. For the 50-HP diesel engine data, the maximum error is 0.0473 or 4.73% of engine design torque, which is adequate for robust control system development. For the 50-HP motor configuration, the vehicle speed response is given in Fig. 18. From this result, it is clear that the traction motor is not large enough to drive the vehicle at the 60-mph reference speed. A steady-state velocity lower than 60-mph is reached when the power losses in the traction motor, coupling, and vehicle dynamics are equal to the AC terminal power in the machine. The steady-state error in this test is 4.2 miles per hour. Several noteworthy facts may also be obtained from Fig. 18. The steady-state velocity is approached asymptotically, but appears to be fairly level at the 150-second mark. Thus, the acceleration in this configuration is fairly low. In contrast, the time to stop from 55.8 mph is 18 seconds. This is of course due to the aerodynamic, viscous, and Coulomb drag in the vehicle dynamics assisting the deceleration. The control variables that produce this result are the traction motor torque and brake torque, shown in Figs. 17 and 15 respectively. The brake torque shown in Fig. 15 is referred to the traction motor shaft for easy comparison with the traction motor torque. In the physical system, this torque is likely to be applied directly at the hub of one or more wheels for maximum efficiency in braking. Finally, the DC current

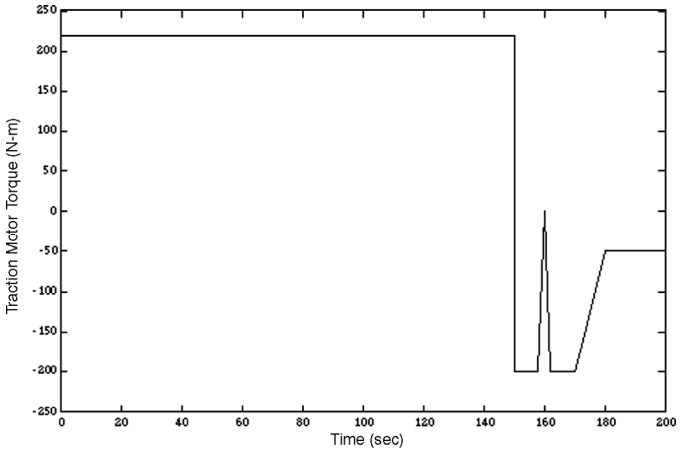

Figure 17. Torque developed in 50-HP traction motor (induction motor).

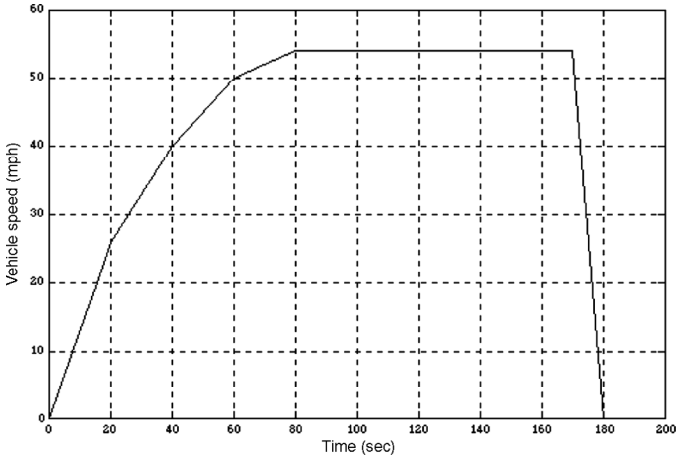

Figure 18. Vehicle speed.

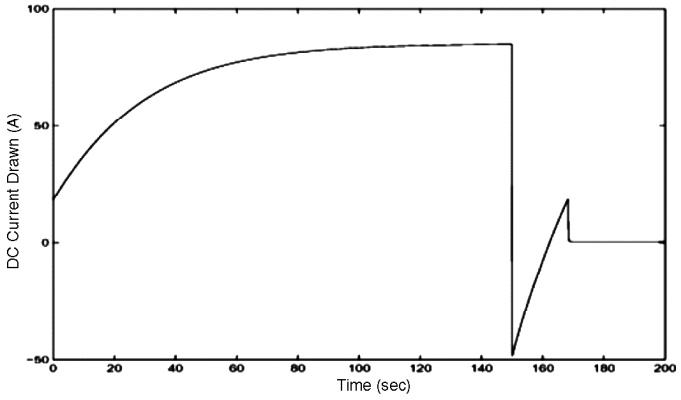

Figure 19. DC current consumption.

required to produce the desired traction motor torque is given in Fig. 19.

7. Conclusion

In this paper, the development and testing procedures of various component models and a system control strategy for a new hybrid vehicle have been proposed. The system model and corresponding SIMULINK code used in this paper are appropriate for long-time-scale simulations in which the dynamics on the order of the electrical frequencies in the machines may be neglected. As such, it has been proven stable for integration time steps up to 0.1 second. The system model has been developed for and is particularly well suited for parametric system studies, in which the main parameters in the vehicle are varied while holding the velocity profile constant as shown in the model using the FUDS driving cycle. To aid in its use as such, an appropriate scaling strategy was presented. Using this strategy, all parameters necessary to simulate the vehicle are scaled from the design power of the engine, the energy capacity of the flywheel battery, and the design power of the traction motor.

8. Nomenclature

i_{ds}	d-axis stator current	Ψ_S	Stator flux linkage
i_{qs}	q-axis stator current	Ψ_{dS}	d-axis stator flux linkage
L_d	d-axis inductance	Ψ_{qS}	q-axis stator flux linkage
L_q	q-axis inductance	Ψ_{dr}	d-axis rotor flux linkage
L_r	Rotor inductance	Ψ_{qr}	q-axis rotor flux linkage
Ls	Stator inductance	T_{em}	Electromagnetic torque
L_m	Mutual inductance	v_s, i_s	Stator voltage and current
R_r	Rotor resistance	R_b	DC bus leakage reactance
R_s	Stator resistance	C_b	DC bus capacitance
ω_r	Angular speed	V_{ds}, V_{qs}	Stator voltages in d and q axes

References

[1] I.R. McNab, Pulsed power parameters, *Institute for Advanced Technology Bulletin*, *1*, 1996, 7–10.

[2] S. Fish, The Institute for Advanced Technology transitions electric combat vehicle modelling tools to DARPA contractors, *Institute for Advanced Technology Bulletin*, *1*, 1996, 18.

[3] K. Yamada, M. Hashiguchi, & M. Ito, Traction control system: Simulation analysis of the control system, *International Journal of Vehicle Design*, *12*(1), 1991, 89–96.

[4] P.C. Krause, *Analysis of electric machinery* (McGraw-Hill, 1986).

[5] I. Boldea & S.A. Nasar, *Vector control of AC drives* (CRC Press, 1992).

[6] T.G. Habetler, F. Profumo, M. Pastorelli, & L.M. Tolbert, Direct torque control of induction machines using space vector modulation, *IEEE Trans. on Industry Applications*, *5*(28), 1992, 1045–1053.

[7] J.–K. Kang, S.–K. Sul, New direct torque control of induction motor for minimum torque ripple and constant switching frequency, *IEEE Trans. on Industry Applications*, *35*(5), 1999, 231–1239.

[8] F.L. Lewis & V.L. Syrmos, *Optimal control* (John Wiley & Sons, 1995).

[9] G.S. Buja & P. Kazmierkowski, Direct torque control of PWM inverter-fed AC motors: A survey, *IEEE Trans. on IE*, *2*(51), 2004, 128–136.

[10] P. Vas, Principles of direct torque control, in *Sensorless vector and direct torque control* (London: Oxford University Press, 1998), 124–253.

[11] *MATLAB: High-performance numeric computation and visualization software*, The Math Works, Inc., Natrick, MA, 2000.

Biographies

M. Vasudevan received his B.E. degree in 1996 and M.E. degree in 1998 from Annamalai University and Bharathidasan University respectively, both in Electrical Engineering. At present, he is a senior manager in the Department of Research and Development in Vestas RRB India Ltd, a wind turbine manufacturing firm in India and working with different ratings of wind electric generators and their controllers. He is the responsible team leader to develop various control algorithms and modules for the controllers. He is pursuing Ph.D. in Anna University, India. He published many papers in International Journals and Conference Proceedings. His research interests include Power Electronics, DSP based induction motor and switched reluctance motor drive, series configured hybrid vehicles and modelling and simulation of adaptive control systems.

R. Arumugam received his B.E. and M.Sc. (Engg) degrees in 1969 and 1971, respectively, from Madras University and his Ph.D. in 1987 from Concordia University, Canada. At present he is professor and head of the Electrical and Electronics Engineering Department, Anna University, India. He has received many research paper awards. His interests include computer-aided design of electrical machines, power electronics, AC motor drives, motor controls, power-factor correction, and magnetic design.

S. Paramasivam received his B.E. degree from GCT, Coimbatore, in 1995 and the M.E. degree from P.S.G. College of Technology, Coimbatore, in 1999, both in Electrical Engineering. He received his Ph.D. from college of Engineering, Guindy, Anna University, India in 2006. At present, he is working in ESAB group, India as a R&D head for equipments and cutting systems. His interests include power electronics, AC motor drives, DSP and FPGA-based motor controls, power-factor correction, and magnetic design and controller design for wind energy conversion systems.